Structured Model Selection for Recovery of Sparse Representations in Nested Periodic Dictionaries

Pouria Saidi
School of Electrical, Computer and Energy Engineering
Arizona State University, Tempe, AZ, 85281 USA.
Email: psaidi@asu.edu

George K. Atia
Department of Electrical and Computer Engineering
Department of Computer Science
University of Central Florida, Orlando, FL, 32816 USA.
Email: george.atia@ucf.edu

2022 56th Asilomar Conference on Signals, Systems, and Computers | 978-1-6654-5906-8/22/$31.00 ©2022 IEEE | DOI: 10.1109/IEEECONF56349.2022.10051897

***Abstract*—Periodic signals were shown to admit sparse representations in Nested periodic dictionaries (NPDs). Therefore, sparse recovery frameworks have been employed to estimate the periodicity in signals by finding their sparse representations in such dictionaries. However, existing sparse recovery algorithms such as Orthogonal Matching Pursuit (OMP) are oblivious to the structure of the dictionary, and as a result their performance degrade in settings involving periodic mixtures. In this work, we propose new algorithms for structured model selection, termed nested periodic subspace OMP and nested periodic subspace regularized OMP, that leverage the well-known Euler structure and LCM property of NPDs. We evaluate the performance of these methods using both synthesized and real data and show that they can yield better performance than generic recovery algorithms while also saving in computation time.**

***Index Terms*—Nested periodic dictionaries, Nested periodic subspace orthogonal matching pursuit, Periodic mixtures**

I. Introduction

Robust period estimation of periodic signals is at the heart of many applications ranging from medicine [1] and healthcare [2], [3] to astrophysics [4]. In many such applications, it is essential to obtain an accurate estimate of the period in real-time. Many of the existing techniques for period estimation are based on the discrete Fourier transform [5], [6]. While the exact fundamental frequency of a periodic signal can be recovered using DFT-based methods when the data length L is a multiple of its period, these methods yield inaccurate estimates in short data length regimes and with arbitrary L [7]. Also, a periodic signal could be the combination of multiple periodic signals. As a result, the resulting period could be larger than the data length. In this case, identifying all the hidden periods in the signal with a short data length could be even more challenging, and methods such as recursive differencing often fail [7]. Furthermore, in real world applications, signals may be quasi-periodic due to the presence of noise, which degrades the performance of spectral-based techniques.

Given these limitations, Tenneti and Vaidyanathan revisited the problem of periodicity estimation in [7], where they introduced a family of matrices called nested periodic dictionaries (NPDs), an instance of which is the so-called Ramanujan periodicity transform (RPT). They have shown that periodic signals admit sparse representation in NPDs. Therefore, one can express a periodic signal using the model

$$\mathbf{y} = \mathbf{K}\mathbf{x}, \tag{1}$$

where $\mathbf{K} \in \mathbb{C}^{L\times N}$ is an NPD, $\mathbf{y}$ is the periodic vector of length L, and $\mathbf{x} \in \mathbb{C}^N$ is its sparse representation. The underlying period of a periodic signal can be estimated by recovering the support set of its sparse representation in an NPD, which motivated the use of sparse recovery frameworks for period estimation [7]–[9]. For instance, [7] proposed an optimization program based on ℓ_2-norm regularization that gives a closed-form solution to recover the sparse vector. The authors in [8] employ a sparse recovery framework based on ℓ_1-norm regularization, and guarantees for sparse recovery using the basis pursuit program were established in [10].

Generic sparse recovery guarantees do not hold for NPDs, which exhibit specific structures, as was shown in [10]. Therefore, [11] established improved support recovery guarantees for periodic signals that incorporate the well-known Euler structure of such dictionaries using basis pursuit and Orthogonal Matching Pursuit (OMP) [12], [13]. While these conditions improve significantly upon the generic sparse recovery conditions (in the sense that they hold over a wider range of the sparsity level), from an algorithmic standpoint, OMP and related algorithms are oblivious to the structure of these dictionaries. In addition, OMP selects only one atom in each iteration, which leads to a large computation time. There have been extensions to the OMP algorithm that select more than one atom in each iteration. For instance, in regularized OMP (ROMP) [14], one can select multiple atoms at once if the magnitude of the inner products between the atoms of the dictionary and the residual of the sparse approximation induced by the model selection meets a pre-defined criteria. Also, the Subspace Pursuit algorithm [15] selects the atoms with the k largest projections followed by a pruning step.

Motivated by the aforementioned limitations, in this work, we develop algorithms that leverage the structural properties of NPDs in their design to enhance the recovery of periodic mixtures, while also reducing the computation time. To the best of our knowledge, this is done here for the first time. In particular, we propose two methods that account for the Euler structure and LCM property of NPDs by enforcing a block-structured representation in our model selection, defined over the union of the support sets of the divisors of the periods in the periodic mixture.

The paper is organized as follows. In Section II, we briefly review necessary background on important properties

of NPDs, and the OMP algorithm. In Section III, we present the proposed methods. The numerical results are provided in Section IV. We conclude the paper in Section V.

A. Notation

We use lowercase letters for scalars, bold lowercase letters for vectors, and bold uppercase letters for matrices. For a vector $\mathbf{v}$ of size l with entries v_i, $\|\mathbf{v}\|_2 := \left(\sum_{i=1}^{l} v_i^2\right)^{1/2}$ denotes its ℓ_2 norm. For an $L \times N$ matrix $\mathbf{A}$ with entries $a_{i,j}$, $\mathbf{A}^H$ is its conjugate-transpose. The set $\mathbb{P} := \{1, \ldots, P_{\max}\}$ is the set of all integers between 1 and $P_{\max}$, where $P_{\max}$ is the largest possible period. For each $p \in \mathbb{P}$, we use $q|p$ to indicate that q is a divisor of p. The Euler totient function $\phi(p)$ of p is the number of positive integers smaller than p that are co-prime to p. Given a set S, $|S|$ denotes its cardinality. The matrix $\mathbf{K}_S$ is the matrix $\mathbf{K}$ restricted to the atoms indexed by set S.

II. Background

A. Nested Periodic Dictionaries

We briefly review the construction and properties of the RPT dictionary as an instance of NPDs. RPT dictionaries are constructed from Ramanujan sums, defined as

$$c_p(n) = \sum_{\substack{k=1 \\ (k,p)=1}}^{p} \exp(j2\pi kn/p), \tag{2}$$

where (k, p) is the greatest common divisor (gcd) of k and p. In (2), $c_p(n)$ is an all integer, periodic sequence with period p. From these sums, one can build a $p \times \phi(p)$ submatrix $\mathbf{C}_p$

$$\mathbf{C}_p = \begin{bmatrix} \mathbf{c}_p & \mathbf{c}_p^{(1)} & \ldots & \mathbf{c}_p^{(\phi(p)-1)} \end{bmatrix}, \tag{3}$$

where $\mathbf{c}_p$ is the vector form of $c_p(n)$ and $\mathbf{c}_p^{(i)}$ is the circularly shifted version of $\mathbf{c}_p$ with step-size i. The columns of $\mathbf{C}_p$ are linearly independent [16]. Then, the RPT dictionary $\mathbf{K}$ can be built by first constructing the submatrices $\mathbf{C}_p$ for all $p \in \mathbb{P}$, then periodically extending them to length L to obtain matrices $\mathbf{R}_p$, and finally concatenating the matrices $\mathbf{R}_p$ as

$$\mathbf{K} = \begin{bmatrix} \mathbf{R}_1 & \mathbf{R}_2 & \ldots & \mathbf{R}_{P_{\max}} \end{bmatrix}. \tag{4}$$

Euler structure and LCM property: Each of the submatrices of the RPT matrix $\mathbf{K}$ contains exactly $\phi(p)$ atoms that are periodic with period p. This is known as the Euler structure of NPDs. Also, given a sufficiently large number of measurements L, a linear combination of atoms of an NPD give rise to a periodic signal with period equal to the least common multiplier (lcm) of the periods of the atoms, which is known as the LCM property [17]. Given these two properties, one can recover the hidden periods of a periodic signal by recovering the exact support of its sparse representation in an NPD [7].

B. Periodic Mixtures

A periodic mixture is a periodic signal formed by combining multiple periodic signals [9]

$$y(n) = y_1(n) + y_2(n) + \ldots + y_m(n), \tag{5}$$

with distinct period $p_1, p_2, \ldots, p_m$. The periods p_j for $j = 1, 2, \ldots, m$ are known as the hidden periods of the mixture. They should not be divisors of one another, and each of the periodic signals $y_j(n)$ cannot be further decomposed into signals of smaller periodicities.

C. Orthogonal Matching Pursuit (OMP)

Given the model in (1), one can use the well-known OMP algorithm [12], [13], [18] to recover the sparse vector $\mathbf{x}$ iteratively. OMP first selects the atom of the dictionary that has the maximum projection with the observation vector $\mathbf{y}$. Subsequently, the process is repeated by iteratively selecting the atom that maximizes the projection with the residual $\mathbf{r}$ of the approximation induced by the set of selected atoms, until the residual is sufficiently small.

III. Methods

In this section, we propose two new algorithms, dubbed nested periodic subspace orthogonal matching pursuit (NS-OMP) and nested periodic subspace regularized OMP (NS-ROMP), to recover the support set of the sparse representation of a periodic mixture in NPDs. NS-OMP and NS-ROMP are presented in Algorithm 1 and Algorithm 2, respectively. The underpinning of these methods is exploiting the Euler structure and LCM property of NPDs. To describe our algorithms, we elaborate on the main components that underlie our approach.

A. Enforcing a Block Structure

The LCM property of the NPDs indicate that the sparse vector $\mathbf{x}$ in (1) is supported on the divisors of the hidden periods. Therefore, because of the Euler structure of the NPDs, we deduce that the sparse representations of the periodic mixtures in an NPD exhibit a block structure. We can express the vector $\mathbf{x}$ and the NPD $\mathbf{K}$ in block forms as

$$\mathbf{x} = \big[\underbrace{x_1}_{\mathbf{x}_1^T}, \underbrace{x_2}_{\mathbf{x}_2^T}, \underbrace{x_3, x_4}_{\mathbf{x}_3^T}, \ldots, \underbrace{x_{N-\phi(P_{max})+1}, \ldots, x_N}_{\mathbf{x}_{P_{\max}}^T}\big]^T \tag{6}$$

and

$$\mathbf{K} = \big[\underbrace{\mathbf{k}_1}_{\mathbf{R}_1}, \underbrace{\mathbf{k}_2}_{\mathbf{R}_2}, \underbrace{\mathbf{k}_3, \mathbf{k}_4}_{\mathbf{R}_3}, \ldots, \underbrace{\mathbf{k}_{N-\phi(P_{\max})+1}, \ldots, \mathbf{k}_N}_{\mathbf{R}_{P_{\max}}}\big]. \tag{7}$$

If p is one of the hidden periods of the given periodic mixture, then all entries $\mathbf{x}_q$ for $q|p$ could be nonzero. We seek to exploit this prior knowledge to improve the support recovery performance for large sparsity levels, as well as the computational efficiency (e.g., number of iterations). To the best of our knowledge, the proposed algorithms are the first to account for structural information of NPDs for sparse recovery. First, we need the following definition, which defines the support set of the submatrices $\mathbf{R}_p$ in the NPD for $p \in \mathbb{P}$.

Definition 1 (Support set)**.** *The index set* $I_p = \{\sum_{j=1}^{p-1} \phi(j) + 1, \ldots, \sum_{j=1}^{p} \phi(j)\}$ *denotes the indices of the* $\phi(p)$ *atoms of an NPD* $\mathbf{K}$ *that have period* p*, i.e., submatrix* $\mathbf{R}_p$ *in* (7)*.*

Let $\mathcal{T} = \{p_1, p_2, \ldots, p_m\}$ be the set of hidden periods of a periodic mixture. Per the LCM property, the nonzero coefficients of the sparse vector $\mathbf{x}$ in (1) are supported on the union of index sets corresponding to the submatrices $\mathbf{R}_q$ for every $q|p_j$ and $p_j \in \mathcal{T}$, given sufficiently many measurements. Thus, $S_{\mathcal{T}} = \bigcup_{q \in D_{\mathcal{T}}} I_q$ contains the support set, where $D_{\mathcal{T}}$ is the set of all divisors of the hidden periods in $\mathcal{T}$. Hence, in Step 3 of the proposed methods, we enforce the block structure by always selecting atoms from the index sets I_p given in Definition 1.

B. Adaptive Model Selection

The standard OMP algorithm discussed in Section II-C selects one atom in each iteration, and ignores any prior information about the structure of the dictionary. Instead, we propose to select an adaptive number of atoms in each iteration following the Euler structure of NPDs. In particular, in Step 3 (item 1) of NS-OMP and NS-ROMP, we find the maximum projection between the residual vector and the atoms in the dictionary, then select all the atoms of the submatrix $\mathbf{R}_p$ that comprises the atom with the largest projection. As shown in (7), these matrices are of different sizes depending on p.

Algorithm 1 NS-OMP

1: **Input**: Observation vector $\mathbf{y}$, NPD $\mathbf{K}$, $P_{\max}$.
2: **Initialization**: Let index set $J_0 = \emptyset$, and residual vector at iteration $t = 0$, to be $\mathbf{r}_0 = \mathbf{y}$.
3: **While** $\|\mathbf{r}_t\|_2 \geq \epsilon$ or $|J_t| \leq k$, $t \leftarrow t + 1$
- At iteration t, find $i^\star = \arg\max_{i \in \{1,\ldots,N\}} \mathbf{k}_i^H \mathbf{r}_{t-1}$. Select the index set I_p which contains $i^\star$ (See Definition 1).
- Update the support set: $J_t = J_{t-1} \bigcup I_p$.
- Let $\mathbf{P}_t = \mathbf{K}_{J_t} \left(\mathbf{K}_{J_t}^H \mathbf{K}_{J_t}\right)^{-1} \mathbf{K}_{J_t}^H$. Update the residual: $\mathbf{r}_t = (\mathbf{I} - \mathbf{P}_t)\,\mathbf{y}$

4: **Output**: The index set J_t.

C. Regularization and Refinement

While the sparse representation of periodic mixtures exhibit a block structure following the Euler structure of NPDs as described above, this does not imply that all the coefficients within the blocks that correspond to the support set must be nonzero. Techniques that select more than one atom in each iteration are prone to over selecting atoms in each iteration. Erroneous selections could propagate to subsequent iterations leading to false model selection. To remedy this, we include a regularization step to limit the number of atoms selected, as well as a refinement step to remove unwanted atoms that were selected in previous iterations. The additional regularization and refinement steps are only included in NS-ROMP, as described in Step 3 (items 2,3) and (item 5) in Algorithm 2, respectively. In the regularization step, we only select a subset of the atoms in $\mathbf{R}_p$ with the largest projections. Specifically, in iteration t, we select the first consecutive indices of V_t that are also in I_p, where V_t is the sorted set of indices corresponding to the largest $|I_p|$ projections and I_p is the support set of submatrix $\mathbf{R}_p$. For refinement, after selecting the atoms in each iteration, we find the estimated sparse vector $\hat{x}$ and only keep those atoms whose coefficients in $\hat{x}$ are greater than a certain threshold in absolute value. Hence, similar to NS-OMP, the NS-ROMP algorithm enforces a block structure and performs adaptive model selection following the Euler structure, but it also continually revisits the selections and removes the unwanted atoms. We remark that a related approach to refinement is used in Subspace Pursuit [15] with the main difference that NS-ROMP is tailored to NPDs as it accounts for their Euler structure. Therefore, the number of atoms it selects before the refinement step is not fixed, and a regularization step ensures that the projection of the atoms on the residual are amongst the largest. Hence, we anticipate a higher success rate for NS-ROMP for periodic mixtures with sparse representations in NPDs, which is verified in our numerical results.

Algorithm 2 NS-ROMP

1: **Input**: Observation vector $\mathbf{y}$, NPD $\mathbf{K}$, $P_{\max}$ and threshold T_x.
2: **Initialization**: Let index set $J_0 = \emptyset$, and residual vector at iteration $t = 0$, to be $\mathbf{r}_0 = \mathbf{y}$.
3: **While** $\|\mathbf{r}_t\|_2 \geq \epsilon$ or $|J_t| \leq k$, $t \leftarrow t + 1$
- At iteration t, find $i^\star = \arg\max_{i \in \{1,\ldots,N\}} \mathbf{k}_i^H \mathbf{r}_{t-1}$. Select the index set I_p, where $i^\star \in I_p$.
- Let $V_t = \{v_1, v_2, \ldots v_{|I_p|}\}$ be the set that contains the $|I_p|$ indices with largest projections $\mathbf{k}_i^H \mathbf{r}_{t-1}$ in a descending order.
- Select the subset $I_v \subseteq V_t$ that consists of the first consecutive indices of V_t that are also in I_p.
- Update the support set: $J_t' = J_{t-1} \bigcup I_v$.
- **Refinement**
  - Find $\mathbf{x}_{J_t'} = \left(\mathbf{K}_{J_t'}^H \mathbf{K}_{J_t'}\right)^{-1} \mathbf{K}_{J_t'}^H \mathbf{y}$
  - $J_t = \{\ell | \ell \in J_t', |x_\ell| > T_x\}$.
- Let $\mathbf{P}_t = \mathbf{K}_{J_t} \left(\mathbf{K}_{J_t}^H \mathbf{K}_{J_t}\right)^{-1} \mathbf{K}_{J_t}^H$. Update the residual: $\mathbf{r}_t = (\mathbf{I} - \mathbf{P}_t)\,\mathbf{y}$

4: **Output**: The index set J_t.

IV. Numerical Results

In this section, we evaluate the performance of NS-OMP and NS-ROMP algorithms using numerical experiments with both synthesized and real data. Also, we compare the performance of these methods to the OMP algorithm [18] and subspace pursuit (SP) [15]. Here, we limit our evaluation to the RPT dictionary, which is an all integer dictionary and allows for faster computations. Note that the values of the hidden periods p_j's and their number m induce signals with different sparsity levels. Hence, to validate the performance

of the proposed methods with respect to a sparsity level, we define the set

$$\mathbb{Q}_k(m) := \{\mathcal{T} \in 2^{\mathbb{P}} : |\mathcal{T}| = m, |S_{\mathcal{T}}| \leq k\}$$

which contains all combinations of m elements of $\mathbb{P}$ that induce a sparsity level k. For example, if $P_{\max} = 20$, $m = 2$ and $k = 6$, then $\mathbb{Q}_6(2) = \{\{2,3\},\{2,5\},\{3,4\},\{3,7\}\}$.

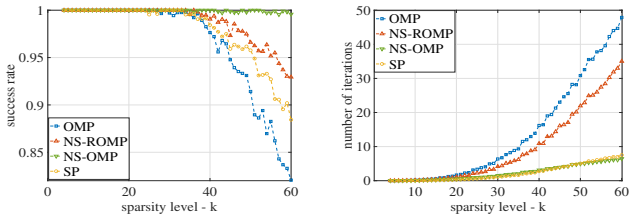

(a) (b)

Fig. 1: Evaluation of NS-ROMP and NS-OMP for Experiment 1 using periodic mixtures from the set $\mathbb{Q}_k(m)$ in comparison to OMP and SP, (a) success rate, (b) number of iterations.

Experiment 1: We start off with periodic mixtures that contain exactly 2 hidden periods. We generate periodic mixtures for each member $\mathcal{T}$ of the set $\mathbb{Q}_k(2)$. To this end, we generate random sequences of length $p_j \in \mathcal{T}$, extend them periodically to length L, and add them to construct the periodic mixture. We evaluate the performance of the proposed methods by reporting the success rate and the average number of iterations. We choose $P_{\max} = 40$ and $L = 200$. As shown in Fig. 1, NS-ROMP outperforms the OMP and SP algorithms maintaining a higher success rate at larger sparsity levels. Also, it does so with a significantly smaller number of iterations than OMP.

Experiment 2: In the second experiment, we highlight the importance of the regularization step in NS-ROMP. We generate sparse vectors with k nonzero coefficients, and use the model in (1) to construct the periodic mixtures. The locations of the k nonzero entries of $\mathbf{x}$ are randomly selected and the nonzero values are drawn from a standard normal distribution. In this case, some of the entries of the sparse vector indexed by set $S_{\mathcal{T}}$ could be zero. For each $\mathbf{x}$, we compare the recovered support set with the known support set and count it as successful support recovery if the two sets are equal. In addition, we report the average number of iterations to reach the solution for each method. We choose $P_{\max} = 40$ and $L = 200$. As shown in Fig. 2a, NS-ROMP maintains a very high success rate for larger sparsity levels k in comparison to OMP and SP. The performance of NS-OMP degrades drastically due to oversampling from each of the submatrices $\mathbf{R}_p$. The performance of NS-ROMP is superior to SP in terms of reaching higher success rate for larger sparsity levels. However, SP required a smaller number of iterations.

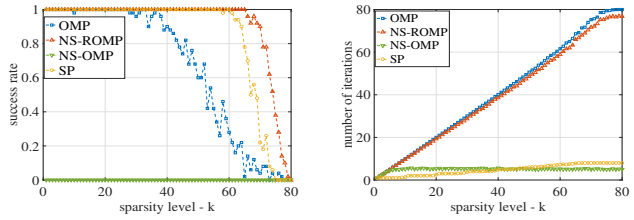

(a) (b)

Fig. 2: Evaluation of NS-OMP and NS-ROMP for Experiment 2 in comparison to OMP and SP, (a) success rate, (b) average number of iterations. The dictionary has $P_{\max} = 40$.

Real data: We examine the ability of the proposed methods to determine the underlying period of ECGs. We use the MIT-BIH normal sinus rhythm database [19] that includes long-term ECG recordings. We extract 10 seconds of ECG recordings and utilize the proposed algorithms and standard OMP to recover the sparse representations of the ECG signals in the RPT dictionary. We expect to observe non-zero coefficients at indices outside the set $S_{\mathcal{T}}$ that we consider to be the exact support set. We compute the energy of the subvectors in $\mathbf{x}$, where each subvector corresponds to one submatrix $\mathbf{R}_p$ in the NPD as follows [7]

$$E(d_i) = \sum_{k=K+1}^{K+\phi(d_i)} |c(k)|^2, \quad K = \sum_{\substack{p|P \\ p<d_i}} \phi(p). \tag{8}$$

We use the greatest energy value to determine the underlying period. Given the sampling frequency of 128 Hz, we compute the heart rate for each 10 seconds window as HR $= 10 \times 128/\hat{p}$, where $\hat{p}$ is the recovered period and HR denotes the heart rate per 10 seconds. To validate the results, we manually extract the rate by counting the number of heartbeats in each 10-second window. Fig. 3 shows the results for two ECG trials. Fig. 3a shows a 10-second window of an ECG trial, and Fig. 3b and Fig. 3c show the corresponding energy vs. period plots where the sparse vector is recovered using OMP and NS-ROMP, respectively. Both graphs suggest that the underlying period is 80, and we can compute the HR $= 16$ beats in each 10 seconds, which can be verified by examining the original ECG signal in Fig. 3a. The computation time to recover the sparse vector using OMP was 3.07 seconds versus 1.42 seconds for NS-ROMP. Fig. 3d shows a 10-second window from another trial. Fig. 3e and 3f show the energies in each period, suggesting that the period $\hat{p} = 99$, hence HR $= 12.92$ beats in 10 seconds. The computation times to recover the sparse vectors are 2.26 and 1.32 seconds using OMP and NS-ROMP, respectively.

V. Conclusion

We proposed two algorithms to recover the sparse representations of periodic mixtures in NPDs. These methods sample an adaptive number of atoms in each iteration by leveraging the properties of NPDs, namely, the Euler structure and the LCM property. The NS-OMP algorithm is superior in comparison to other methods when the actual support set is exactly equal to $S_{\mathcal{T}}$, the union of the support sets of the divisors of the hidden periods. However, the performance of

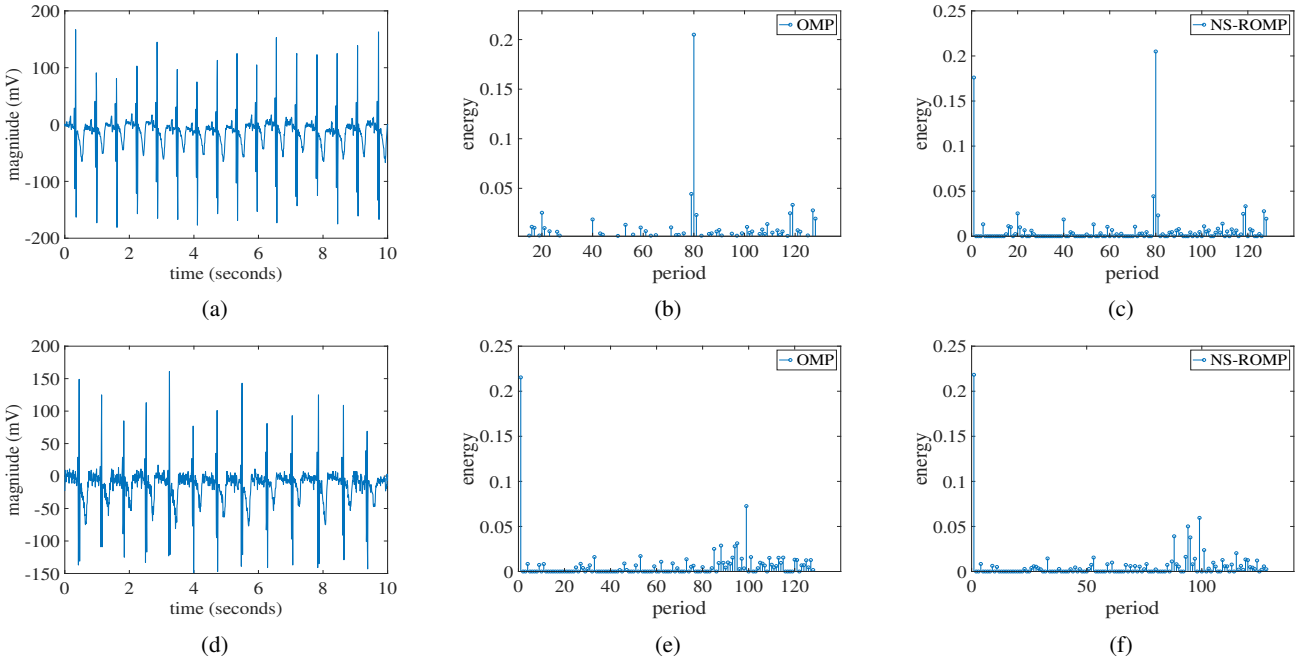

Fig. 3: Numerical results with real data. (a) An ECG trial with 16 beats in 10 seconds. (d) An ECG trial with 13 beats in 10 seconds. (b),(e) The energy vs. period plots based on the recovered sparse vector using OMP and (c),(f) NS-ROMP.

the algorithm deteriorates when the support set is a proper subset of $S_{\mathcal{T}}$. Our numerical results on synthesized data show that NS-ROMP can achieve higher success rate than the OMP algorithm while using a smaller number of iterations. Furthermore, experiments with real ECG data show that the NS-ROMP method can successfully estimate the heart rate.

ACKNOWLEDGMENTS

This work was supported in part by NSF CAREER Award CCF-1552497 and NSF Award CCF-2106339.

REFERENCES

[1] S. V. Tenneti and P. P. Vaidyanathan, "Detecting tandem repeats in DNA using Ramanujan filter bank," in *IEEE International Symposium on Circuits and Systems (ISCAS)*, 2016, pp. 21–24.

[2] G. Da Poian, C. J. Rozell, R. Bernardini, R. Rinaldo, and G. D. Clifford, "Matched filtering for heart rate estimation on compressive sensing ECG measurements," *IEEE Transactions on Biomedical Engineering*, vol. 65, no. 6, pp. 1349–1358, 2017.

[3] P. Saidi, A. Vosoughi, and G. K. Atia, "Detection of brain stimuli using Ramanujan periodicity transforms," *Journal of Neural Engineering*, vol. 16, no. 3, pp. 036021, 2019.

[4] A. Hewish, S. J. Bell, J. D. H. Pilkington, P. F. Scott, and R. A. Collins, "Observation of a rapidly pulsating radio source," in *A Source Book in Astronomy and Astrophysics, 1900–1975*, pp. 498–504. Harvard University Press, 2013.

[5] J. D. Wise, J. Caprio, and T. W. Parks, "Maximum likelihood pitch estimation," *IEEE Transactions on Acoustics, Speech, and Signal Processing*, vol. 24, no. 5, pp. 418–423, 1976.

[6] M. G. Christensen, A. Jakobsson, and S. H. Jensen, "Joint high-resolution fundamental frequency and order estimation," *IEEE Transactions on Audio, Speech, and Language Processing*, vol. 15, no. 5, pp. 1635–1644, 2007.

[7] S. V. Tenneti and P. P. Vaidyanathan, "Nested periodic matrices and dictionaries: New signal representations for period estimation," *IEEE Transactions on Signal Processing*, vol. 63, no. 14, pp. 3736–3750, 2015.

[8] P. P. Vaidyanathan and P. Pal, "The Farey-dictionary for sparse representation of periodic signals," in *IEEE International Conference on Acoustics, Speech and Signal Processing (ICASSP)*, 2014, pp. 360–364.

[9] S. V. Tenneti and P. P. Vaidyanathan, "Minimum data length for integer period estimation," *IEEE Transactions on Signal Processing*, vol. 66, no. 10, pp. 2733–2745, 2018.

[10] P. Saidi and G. K. Atia, "Sparse recovery guarantees of periodic signals with nested periodic dictionaries," in *IEEE Information Theory Workshop (ITW)*, 2021.

[11] P. Saidi and G. K. Atia, "Support recovery guarantees for periodic signals with nested periodic dictionaries," *arXiv preprint arXiv:2110.13200*, 2021.

[12] Y. C. Pati, R. Rezaiifar, and P. S. Krishnaprasad, "Orthogonal matching pursuit: Recursive function approximation with applications to wavelet decomposition," in *Proceedings of 27th Asilomar conference on signals, systems and computers*. IEEE, 1993, pp. 40–44.

[13] G. M. Davis, S. G. Mallat, and Z. Zhang, "Adaptive time-frequency decompositions," *Optical engineering*, vol. 33, no. 7, pp. 2183–2191, 1994.

[14] D. Needell and R. Vershynin, "Uniform uncertainty principle and signal recovery via regularized orthogonal matching pursuit," *Foundations of computational mathematics*, vol. 9, no. 3, pp. 317–334, 2009.

[15] W. Dai and O. Milenkovic, "Subspace pursuit for compressive sensing signal reconstruction," *IEEE transactions on Information Theory*, vol. 55, no. 5, pp. 2230–2249, 2009.

[16] P. P. Vaidyanathan, "Ramanujan sums in the context of signal processing—part I : Fundamentals," *IEEE Transactions on Signal Processing*, vol. 62, no. 16, pp. 4145–4157, 2014.

[17] S. V. Tenneti and P. P. Vaidyanathan, "A unified theory of union of subspaces representations for period estimation," *IEEE Transactions on Signal Processing*, vol. 64, no. 20, pp. 5217–5231, 2016.

[18] J. A. Tropp, "Greed is good: Algorithmic results for sparse approximation," *IEEE Transactions on Information Theory*, vol. 50, no. 10, pp. 2231–2242, 2004.

[19] A. L. Goldberger, L. A. Amaral, L. Glass, J. M. Hausdorff, P. Ch. Ivanov, R. G. Mark, J. E. Mietus, G. B. Moody, Ch. Peng, and H. E. Stanley, "Physiobank, physiotoolkit, and physionet: components of a new research resource for complex physiologic signals," *circulation*, vol. 101, no. 23, pp. e215–e220, 2000.